IOP Publishing Nanotechnology
Nanotechnology 30 (2019) 095701 (8pp) https://doi.org/10.1088/1361-6528/aaf7cc

Polymer spreading on substrates with nanoscale grooves using molecular dynamics

Brooklyn A Noble and Bart Raeymaekers

Department of Mechanical Engineering, University of Utah, Salt Lake City, UT 84112, United States of America

E-mail: bart.raeymaekers@utah.edu

Received 22 September 2018, revised 17 November 2018
Accepted for publication 11 December 2018
Published 4 January 2019

Abstract

Understanding how liquid polymer interacts with and spreads on surfaces with nanoscale texture features is crucial for designing complex nanoscale systems. We use molecular dynamics to simulate different types of polymer as they spread on substrates with a single nanoscale groove. We study how groove design affects the potential energy of a substrate and how this governs polymer spreading and orientation. Based on our simulations, we show that groove shape, polymer chemistry, and polymer molecule entanglement are the three parameters that determine polymer spreading on a nanoscale groove. We provide a molecular-level explanation of the underlying physical mechanisms, and we illustrate this fundamental understanding by designing a network of grooves to engineer user-specified polymer spreading and coverage. This work has implications for nanoscale systems and devices that involve the design of complex groove networks with an ultrathin polymer coating, including micro and nanoelectromechanical devices, nanoimprint lithography, flexible electronics, antibiofouling coatings, and hard disk drives.

Supplementary material for this article is available online

Keywords: polymer spreading, nanoscale groove, perfluoropolyether, molecular dynamics simulation

(Some figures may appear in colour only in the online journal)

1. Introduction

Ultrathin liquid polymer films are crucial to the functionality of numerous applications and serve as protective lubricant coatings on hard disk drives [1], antibiofouling coatings for medical devices [2, 3], and are an integral part of many nanoscale manufacturing processes [4], among many others. However, controlling spreading and coverage of an ultrathin liquid polymer film is challenging because surface forces, as opposed to body forces like gravity, dominate on the nanoscale. Several research groups, including ours, have studied polymer spreading on a flat substrate [5–9], whereas only a few research groups have studied polymer spreading on a surface with nanoscale topographical features, despite evidence that such features significantly affect polymer spreading.

Researchers have documented, both experimentally and numerically, and for a variety of solid/liquid systems, that substrates with a pattern of unidirectional grooves can cause anisotropic spreading [10–13], anisotropic wetting [11, 13], and enhanced polymer retention or reflow [14, 15]. Experimental works have documented such observations on surfaces with unidirectional grooves of various shape and size. Zhang *et al* [10] showed that perfluoropolyether (PFPE) polymer spread predominantly along 30 or 50 nm deep unidirectional rectangular grooves on polycarbonate substrates and that spreading decreased with increasing polymer molecular weight. Khare *et al* [11] observed anisotropic wetting and fluidic transport of glycerin droplets on soft polydimethylsiloxane substrates with 500 nm deep unidirectional sinusoidal grooves. They observed that the contact line between the liquid and solid advanced in a

pinning-depinning-repinning manner and suggested that the liquid experienced the presence of energy barriers imposed by the nanoscale features. Fukuzawa *et al* [16] explored this concept further by patterning a silicon substrate with 2.5 nm oxide ridges, which locally altered the wettability of 10 nm PFPE films. They found that in addition to the surface energy of the liquid/air and liquid/solid interfaces, wettability was determined by the intermolecular interaction between the liquid and solid, which even dominated capillary pressure.

Numerical studies have supplemented experiments, which become increasingly difficult with decreasing scale. Zhang *et al* [12] used Monte Carlo simulations to show that the polymer spreading rate increases when approaching the edges of rectangular grooves, and they intuitively attributed this to the increased surface force inside a groove, which is surrounded by as many as three surfaces. Hirvi *et al* [13] employed molecular dynamics (MD) to simulate the wetting of water droplets on polyvinyl chloride surfaces with 0.369–3.070 nm deep rectangular grooves and observed anisotropic spreading with a corrugated contact line where water molecules spread further along the grooves than perpendicular to the grooves. They explained that the nanoscale features confine the droplet radius in the direction perpendicular to the grooves, acting as an energy barrier.

Comparing published works that study liquid spreading on substrates with unidirectional nanoscale grooves, we find that similar observations are documented for different substrates, groove shapes, and liquids, using both simulations and experiments. However, some researchers explain that liquid spreading is accelerated along a groove [10, 12], whereas others describe an energy barrier that seemingly confines spreading perpendicular to the groove direction [11, 13, 16].

Although crucial to the design of ultrathin liquid polymer films for use in engineering applications, no comprehensive understanding of the physical mechanisms that govern liquid polymer spreading in the presence of nanoscale texture features, particularly grooves, seems to exist. This paper provides a molecular-level explanation of liquid polymer spreading on a substrate with a nanoscale groove. We use MD simulations to: (1) quantify how nanoscale groove shape affects polymer spreading, (2) describe the physical mechanisms underlying ultrathin polymer film spreading in a nanoscale groove, and (3) design a network of nanoscale grooves to control spreading for user-specified polymer coverage. We specifically focus on substrates with a single nanoscale groove. We show that anisotropic polymer spreading on a substrate with nanoscale grooves is not due solely to energy barriers that confine the contact line in the direction perpendicular to grooves, as others have previously suggested. Instead, we show that anisotropic spreading can exist within a single groove, and we demonstrate that groove shape determines the degree of anisotropic spreading. Although it has been previously postulated, we quantify how the edge of a groove causes anisotropic spreading and polymer alignment such that we can predict and control spreading.

2. Methods

We perform MD simulations of liquid polymer spreading on a flat substrate and substrates with a triangle, square, or wave-shaped groove using a coarse-grained bead-spring (CGBS) model and the large-scale atomic/molecular massively parallel simulator [17, 18]. The CGBS model averages atomic interactions for computational simplicity yet preserves the essence of the molecular structure. We consider two types of PFPE polymer commonly used in micro- and nanoscale devices, both of which have a backbone structure of X–[(O–CF_2–CF_2)$_p$–(O–CF_2)$_q$]–O–X ($p/q \cong 2/3$): a Zdol molecule, which terminates with a functional hydroxyl group (X = CF_2–CH_2–OH), and a Z molecule, which terminates with a nonfunctional trifluoromethyl group ($X = CF_3$). We vary the polymer molecule length $10 \leqslant N \leqslant 400$ beads for both polymer types while maintaining a constant bead mass of 0.2 kg mol^{-1}, thus varying the molecular weight $2 \leqslant M \leqslant 80$ kg mol^{-1}. The substrate consists of three rigid layers of nonfunctional beads and a fraction of functional beads $0\% \leqslant S_f \leqslant 100\%$ on the top layer only, which strongly attract the functional polymer end beads of Zdol. The potential function interactions are similar to validated potentials used in previous research [7–9, 19–21] and are discussed in detail in the supplementary information, which is available online at stacks.iop.org/NANO/30/095701/mmedia.

We use a quasi-random distribution [22] to define the initial position of the first bead of every polymer molecule and use a random walk approach to define the initial position of the additional beads belonging to each molecule, starting from the first bead. The polymer is free to move according to the microcanonical ensemble, and we hold the temperature constant at 300 K using a Langevin thermostat. The polymer equilibrates within a 23 nm diameter cylinder for at least 7 ns, which represents the pipet used in experiments to deposit a polymer droplet on a substrate. During equilibration, the potential energy of the system initially increases before approaching a constant value. We then remove the cylinder and the polymer spreads on the substrate for approximately 200 ns. We use a timestep of 0.03 ps throughout all MD simulations. The substrate is rigid, and we impose periodic boundary conditions around the simulation box, although the polymer does not cross any boundary during any simulation in this work.

3. Results and discussion

3.1. Groove shape

Figure 1 illustrates spreading of short ($N = 10$, $M =$ 2 kg mol^{-1}), functional polymer (Zdol) on nonfunctional substrates ($S_f = 0\%$) with different groove shapes. (a) a flat substrate, (b) a triangular groove with $\theta = 60°$, (c) a wave groove (one period of a cosine wave), and (d) a square groove. All MD simulation parameters remain constant except the groove shape. For each groove shape, we show the spreading distance parallel to the groove $d_{||}$ (blue square

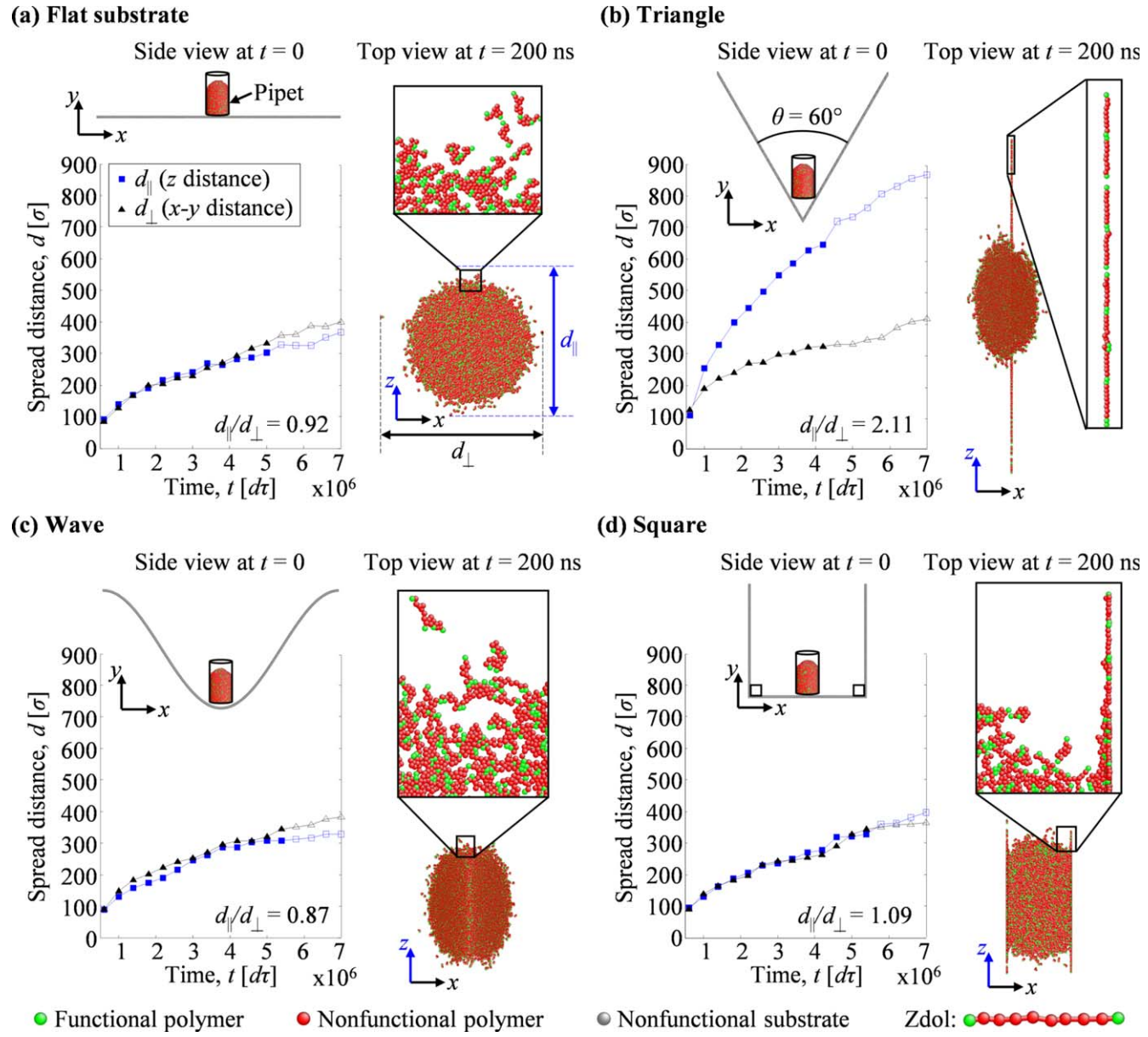

Figure 1. Spreading parallel to the groove $d_{||}$ (blue square markers) and spreading perpendicular to the groove $d_{\perp}$ (black triangle markers) as a function of spreading time for short, functional polymer on nonfunctional substrates with different shapes: (a) flat substrate, (b) triangular groove (c) wave groove, and (d) square groove. Insets show the simulation in the x–y plane (side view) just before spreading and in the x–z plane (top view) after 200 ns, including a magnified view of polymer molecules.

markers) and perpendicular to the groove $d_{\perp}$ (black triangle markers) as a function of spreading time, where 7×10^6 timesteps $d\tau$ corresponds to approximately 200 ns of spreading. Note that the spreading distance perpendicular to the groove is the maximum distance the polymer spreads along the length of the substrate in the x–y plane, which is different from the apparent spreading distance obtained from a projection onto the x–z plane. We quantify spreading parallel to the groove as the polymer spreading distance in the z-direction, i.e. along the groove. We simultaneously evaluate the polymer thickness to determine whether a central droplet exists, which we define as a polymer thickness greater than the 3σ precursor film, where σ is the diameter of one bead. Solid markers indicate that a central droplet exists and hollow markers indicate that the central droplet has depleted. For each groove shape, we show inset images that illustrate the simulation in the x–y plane (side view) just before spreading and in the x–z plane (top view) after 200 ns of spreading, including a magnified view of polymer molecules. The substrate is invisible in the top view for clarity.

From figure 1 we observe that each droplet spreads to a thin film and that $d_{\perp} \simeq 400\sigma$ after 200 ns (black triangle markers), independent of the groove shape. Because $d_{\perp}$ is approximately the same for the flat substrate and substrates with a nanoscale groove, we show that a single groove does not inhibit spreading perpendicular to the groove direction. For the flat, wave, and square grooves, $d_{||}$ is similar to $d_{\perp}$ and also approaches 400σ after 200 ns, i.e. $d_{||}/d_{\perp} \simeq 1$, indicating

isotropic spreading. However, for the triangular groove, polymer spreads more than double in the direction parallel as opposed to perpendicular to the groove, i.e. $d_{||}/d_{\perp} > 2$. Thus, anisotropic spreading may occur with only a single groove because spreading is accelerated parallel to the groove direction, even though spreading is not inhibited perpendicular to the groove direction. The magnified insets of polymer in the x–z plane after 200 ns show that spreading occurs primarily where the groove forms a sharp edge, e.g. the 90° and 60° edges of the square and triangular grooves, respectively. We also observe that the polymer molecules align with the groove at these edges, whereas for the flat substrate and wave groove, polymer molecules do not orient in any particular direction. Thus, the polymer molecules at the edges of the triangular and square grooves are smectic in phase, as the polymer molecules orient parallel and in a well-defined plane. This observation agrees with that of Zhang *et al* [10, 12] who showed that polymer spreading is affected by the edge of groove features. We explain these observations and the anisotropic polymer spreading in the triangular groove based on the potential energy associated with each groove shape.

Figures 2(a)–(d) show 2D spatial potential energy maps on the left and 2D views of the polymer beads (gray dots) and substrate beads (black dots) on the right, projected on the x–y plane after 200 ns, for each of the groove shapes shown in figure 1. We only show the location where spreading parallel to the groove is maximum, which corresponds to the location where the substrate forms a sharp edge (in the case of a rectangular or triangular groove) and where the potential energy is minimum. The spatial potential energy maps display the superposition of the Lennard Jones energy potential of each individual substrate bead, which represents the Van der Waals attraction between a polymer bead and a substrate bead (see supplementary information equation (3)).

From figure 2 we observe that energy wells exist where the attractive energy potentials of multiple substrate beads superimpose (dark blue regions), and polymer beads cluster in these regions to minimize their energy state. When a flat substrate is formed into a nanoscale groove, substrate beads are closely packed where the groove forms a sharp edge. The superposition of energy potentials of substrate beads causes polymer beads to attract to the sharp edge of the groove, which causes the anisotropic polymer spreading documented in figure 1, and agrees with Zhang *et al* [10, 12]. We quantify the magnitude of the energy well created by the different groove shapes as the maximum potential energy range, measured from the minimum potential energy, that defines a spatial region in which the number of polymer beads does not increase by more than 20% with increasing potential energy (see the supplementary information for details and an example calculation of an energy well). For each groove shape in figure 2, we provide the maximum potential energy range that defines the energy well, which we outline with magenta on the spatial potential energy map, and we color the polymer beads contained within the energy well in magenta in the 2D view. Note that the flat substrate has multiple energy wells, all equal in strength, though only one is highlighted with magenta; nanoscale grooves yield a distinct energy well.

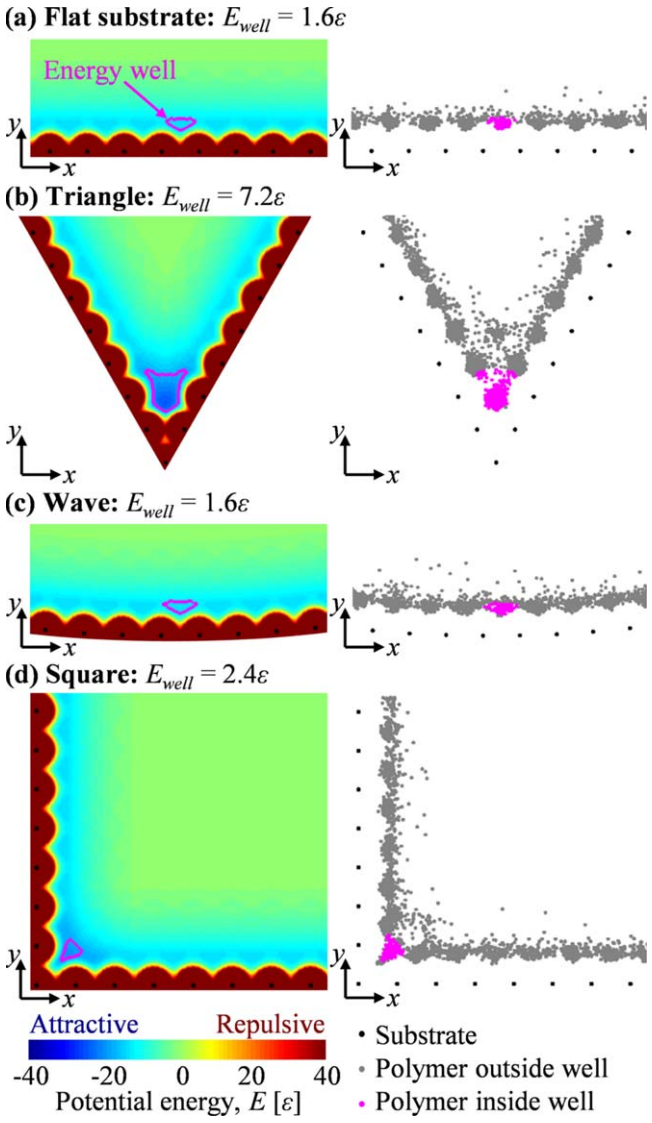

Figure 2. Spatial potential energy map (left) and bead locations in the x–y plane after 200 ns (right) for short, functional polymer on nonfunctional substrates with different shapes: (a) flat substrate, (b) triangular groove (c) wave groove, and (d) square groove. The energy well is outlined with magenta.

We observe that, for a particular substrate, the magnitude of the energy well correlates with the amount of anisotropic spreading. For example, the magnitude of the energy well is approximately the same ($E_{well} = 1.6\varepsilon$) for the flat substrate (figure 2(a)) and wave groove (figure 2(b)), and we observe isotropic spreading on both substrates. For the triangular groove, the magnitude of the energy well is approximately five times larger ($E_{well} = 7.2\varepsilon$) and the spreading distance parallel to the groove is two times larger than for the latter two shapes. We further describe the relationship between the magnitude of the energy well and spreading distance by evaluating the effect of the angle of the triangular groove.

Figure 3 shows polymer spreading parallel (red square markers) and perpendicular (black triangle markers) to triangular grooves with $60 \leqslant \theta \leqslant 180°$ for short ($N = 10$, $M = 2\,\mathrm{kg\,mol^{-1}}$), functional polymer (Zdol) on nonfunctional ($S_f = 0\%$) substrates after 200 ns. Figure 3 also shows the

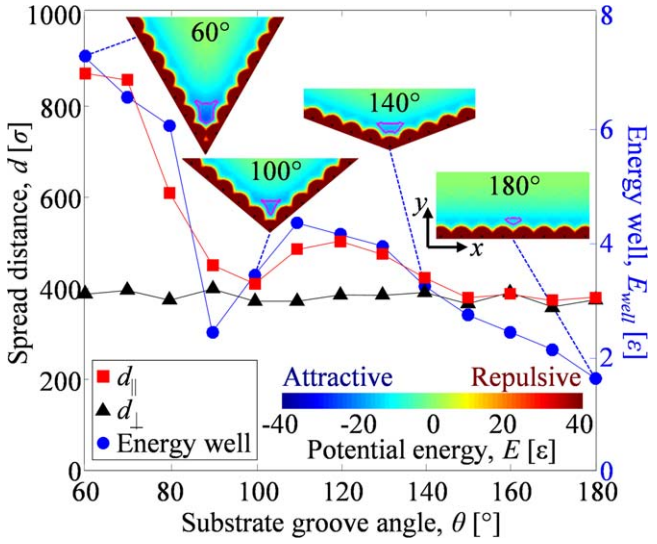

Figure 3. Polymer spreading distance parallel to the groove (red square markers) and perpendicular to the groove (black triangle markers) after 200 ns and the magnitude of the energy well of each substrate (blue circle markers) as a function of triangular groove angle for short, functional polymer molecules on nonfunctional substrates. Insets show spatial potential energy maps for select groove angles with the energy wells outlined in magenta.

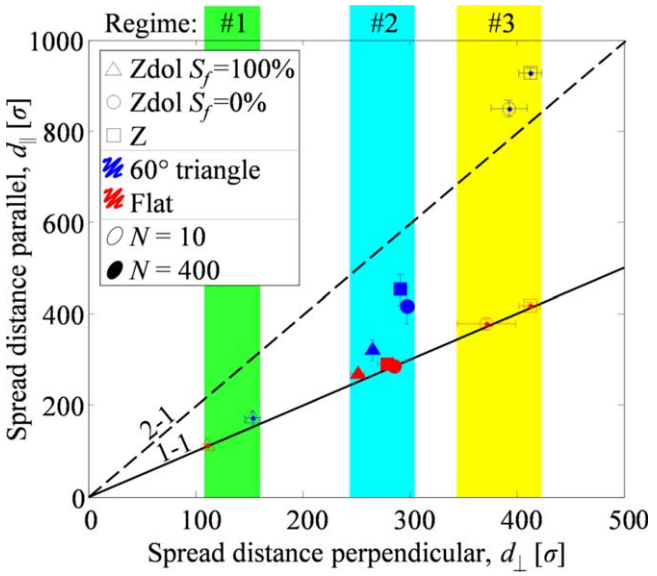

Figure 4. Polymer spreading distance parallel versus perpendicular to the groove after 200 ns for twelve simulations that represent the extremes of parameters studied. The 1–1 line indicates equal spreading in each direction and the 2–1 dashed line indicates spreading twice as far in the direction parallel to the groove compared to the direction perpendicular to the groove. Three distinct spreading regimes are identified.

magnitude of the energy well (blue circle markers). All MD simulation parameters remain constant except the substrate angle. Each simulation was repeated three times, and we report the average. A triangular groove of 60° is the smallest angle we consider because a smaller angle results in overlapping substrate beads at the edge of the groove. Insets show spatial potential energy maps for select triangular groove angles with the energy wells outlined in magenta.

From figure 3 we observe that $d_{\perp}$ is independent of the triangular groove angle. In contrast, $d_{||}$ is a nonlinear function of the triangular groove angle such that a global and local maximum exist at 60° and 120°, respectively. For $90 \leqslant \theta \leqslant 100°$ and $140 \leqslant \theta \leqslant 180°$, we observe that the $d_{||}$ and $d_{\perp}$ are similar and, thus, result in nearly isotropic spreading. The magnitude of the energy well E_{well} also varies nonlinearly with θ and shows a similar trend as the relationship between $d_{||}$ and θ. The correlation coefficient between $d_{||}$ and E_{well} is 0.93, indicating that polymer spreading parallel to the groove is dependent on the angle of the triangular groove. Thus, for short Zdol polymer on nonfunctional substrates, the magnitude of the energy well controls the strength with which polymer beads attract to the groove, promoting polymer spreading in the groove but not affecting spreading perpendicular to the groove.

Thus, we demonstrate that groove shape significantly affects the degree of anisotropic spreading. Potential energy maps reveal the underlying mechanism as potential energy wells that promote spreading along a groove. Furthermore, these potential energy wells vary with groove shape such that a specific spreading behavior can be engineered. Many more groove designs exist that are not included in this study. However, with a specific application in mind, a potential energy map allows evaluating the strength of the potential energy well for any specific groove design.

3.2. Modes of polymer spreading

We compare the physical mechanisms that drive ultrathin polymer film spreading in a nanoscale groove to those that exist on a flat substrate, which we documented in previous work [7]. Figure 4 shows the polymer spreading distance parallel versus perpendicular to the groove after 200 ns for twelve simulations that represent the extremes of parameters we evaluate. Triangle markers indicate functional polymer (Zdol) on a functional substrate ($S_f = 100\%$), circle markers indicate functional polymer on a nonfunctional substrate ($S_f = 0\%$), and square markers indicate nonfunctional polymer (Z). Blue and red markers indicate a triangular groove with $\theta = 60°$ and a flat substrate, respectively. We select these substrates because a triangular groove with $\theta = 60°$ yields the most anisotropic spreading for short, functional polymer on a nonfunctional substrate, whereas the flat substrate yields isotropic spreading. Hollow and solid markers indicate short ($N = 10$, $M = 2\,\mathrm{kg\,mol^{-1}}$) and long ($N = 400$, $M = 80\,\mathrm{kg\,mol^{-1}}$) polymer molecules, respectively. We repeat each simulation twice and report the average, where error bars show the minimum and maximum. Two lines are plotted for reference: the 1–1 line indicates isotropic polymer spreading and the 2–1 dashed line indicates twice as much spreading in the direction parallel compared to perpendicular to the groove.

From figure 4 we observe that isotropic polymer spreading occurs on the flat substrate, as expected (red markers are located near the 1–1 line). We also observe that short,

functional polymer on a functional substrate spreads approximately 100σ in each direction, whereas short, nonfunctional polymer spreads approximately 400σ in each direction. This is in agreement with our previous work on the spreading kinetics of liquid polymer on flat substrates where we identified three spreading regimes based on competing physical mechanisms [7].

Similar to polymer spreading on a flat substrate, we find that polymer spreading in a nanoscale groove can be categorized into three regimes, marked with colored regions in figure 4. The green region represents pressure driven, chemically inhibited flow and applies to short, functional polymer on a functional substrate. In this regime, spreading is inhibited by the chemical attraction of functional polymer end beads to the functional substrate. Regardless of the presence of a groove, we observe nearly isotropic spreading in this regime.

The cyan region represents pressure driven, entanglement inhibited flow and applies to long, functional and nonfunctional polymer molecules. All solid markers fall within this region. In this regime, spreading is inhibited by entanglement of long polymer molecules. Each of these simulations yields an entanglement index $EI > 5$, where the entanglement index is defined as the average number of polymer beads that remain within 2σ of each other for at least 100 000 timesteps [7, 23]. Note that $EI \approx 4$ indicates molecules are largely untangled because the presence of persistent contacts from adjacent polymer beads of the same molecule cause an $EI > 0$. Polymer spreading is still affected by the triangular groove with $\theta = 60°$, resulting in some anisotropic spreading $1 < d_{||}/d_{\perp} < 2$. This result is in agreement with experiments of Zhang *et al* [10] that show anisotropic spreading decreases with increasing molecular weight.

The yellow region represents pressure driven flow with no inhibiting mechanism and applies to short, functional or nonfunctional polymer on a nonfunctional substrate. The polymer molecules do not remain entangled because a molecule length of $N = 10$ is below the critical entanglement length, initially established for a primitive chain by Kremer *et al* [24] and previously identified for our model as $N \approx 20$ [7–9]. In this regime, spreading is most affected by the triangular groove with $\theta = 60°$, resulting in $d_{||}/d_{\perp} > 2$ such that polymer spreads more than twice as much parallel than perpendicular to the groove.

We have previously demonstrated that polymer spreading on a flat substrate does not follow a simple diffusion law, but instead one or more spreading regimes may exist that are attributed to competing physical mechanisms: a pressure difference in the polymer droplet, entanglement of polymer molecules, and attraction of functional chemical groups [7]. The presence of these physical mechanisms depends on polymer type, polymer length, and substrate composition. We find that polymer spreading in a groove and on a flat substrate are governed by the same physical mechanisms. Thus, even for groove geometries that yield a strong energy well, anisotropic spreading does not always occur because spreading is affected by other parameters such as polymer length, polymer type, and functional substrate fraction such that, for some cases, the intermolecular interactions within the polymer dominate the interactions between the polymer and the substrate. As such, we observe less spreading for long polymer molecules on all substrates due to entanglement, and we observe significantly less spreading for short functional polymer on functional substrates due to the attraction of chemical groups. For long polymer molecules, we also observe the most variability in spreading distance because entanglement dominates spreading, and a random component is inherently associated with this regime.

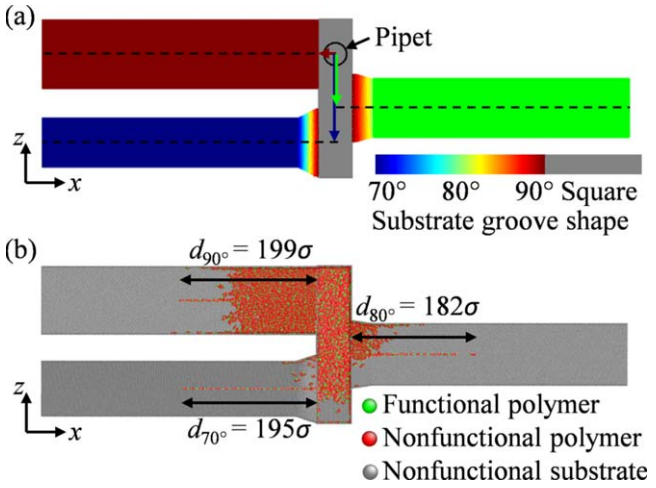

Figure 5. (a) Top view of groove network design that consists of a main square groove and three adjoining triangular grooves. The black circle indicates where the polymer first equilibrates within a cylindrical pipet. (b) Top view of groove network simulation after 200 ns of polymer spreading.

3.3. Groove network design

To apply our understanding of the physical mechanisms that govern polymer spreading in a nanoscale groove, we show an example of how to design a nanoscale groove network to control polymer spreading for user-specified polymer coverage. Specifically, we design a network of grooves such that after 200 ns, polymer spreads 200σ along each groove. Figure 5(a) shows a top view of the network of grooves we designed, which consists of a main square groove (gray) and three triangular grooves adjoining the main groove with groove angles of 70° (blue), 80° (green), or 90° (red). For the 70° and 80° grooves, a 30σ transition from 90° exists for practical purposes. The black circle indicates where the polymer first equilibrates within a cylindrical pipet.

We examine the polymer spreading in the individual triangular grooves with angles of 70°, 80°, and 90° to determine the time required to spread 200σ along each triangular groove. From this, we determine the time allotted to spread in the square groove in order to reach each triangular groove at the appropriate time. Then, we examine the polymer spreading in the square groove to determine the distance allotted between the triangular grooves such that polymer reached each triangular groove at the appropriate time. In figure 5(a), blue, green, and red arrows indicate the paths for the 70°, 80°, and 90° grooves, respectively.

Figure 5(b) shows a top view of the simulation shown in figure 5(a) after 200 ns of spreading. The spreading distance of the polymer along each groove is $d_{90°} = 199\sigma$, $d_{80°} = 182\sigma$, and $d_{70°} = 195\sigma$, thus achieving the objective of spreading approximately 200σ along each groove. Repeating this simulation three times, we quantify the error of the polymer spreading distance along each groove as 6%–10%. By understanding how polymer spreads in a single groove, we can design a network of grooves to engineer and control polymer spreading and coverage on a substrate by changing only the substrate groove design. As such, nanoscale grooves enable engineering spreading such that the following can be obtained: anisotropic polymer spreading using only a nanoscale groove, increased spreading along a groove for applications where polymer film depletion is a problem, or a user-specified polymer spreading or coverage pattern using groove networks. This research is relevant to many engineering applications and research fields where control of ultrathin liquid polymer films on solid surfaces is desirable, including tribology, manufacturing, and interface science, among others.

4. Conclusions

We show that anisotropic polymer spreading on a substrate with nanoscale grooves is not due solely to energy barriers that confine the contact line in the direction perpendicular to grooves, as others have previously suggested. Instead, when a groove exhibits a sharp edge, the intermolecular forces between the polymer and substrate dominate to yield anisotropic spreading that is preferential in the direction parallel to the groove. Three factors determine if anisotropic polymer spreading occurs: (1) substrate geometry (groove shape), (2) chemical end groups of the polymer (Z or Zdol), and (3) polymer molecule length. The groove design affects spreading because the energy potentials of closely packed substrate beads at the edge of the groove superimpose to strongly attract polymer beads. The energy well at the edge of the groove promotes polymer to spread parallel to the groove without affecting spreading perpendicular to the groove because polymer molecules cluster where the energy is strongly attractive to minimize their energy state. Quantifying the magnitude of energy wells enables predicting polymer spreading. Triangular substrates with angles $60 \leqslant \theta \leqslant 80°$ and $110 \leqslant \theta \leqslant 130°$ yield a strong energy well, which leads to anisotropic spreading unless inhibited by the attraction of chemical groups to the substrate or the entanglement of long polymer molecules.

Acknowledgments

This work used the Extreme Science and Engineering Discovery Environment (XSEDE) Comet at the San Diego Supercomputer Center through allocation MSS150011, which is supported by the National Science Foundation grant number ACI-1053575. The support and resources from the Center for High Performance Computing at the University of Utah are gratefully acknowledged. Brooklyn Noble also gratefully acknowledges the Department of Energy Stewardship Science Graduate Fellowship program support, provided under grant number DE-NA0003864.

ORCID iDs

Bart Raeymaekers https://orcid.org/0000-0001-5902-3782

References

[1] Marchon B 2009 Lubricant design attributes for subnanometer head-disk clearance *IEEE Trans. Magn.* **45** 872–6
[2] Maitz M F 2015 Applications of synthetic polymers in clinical medicine *Biosurface Biotribology* **1** 161–76
[3] Epstein A K, Wong T-S, Belisle R A, Boggs E M and Aizenberg J 2012 Liquid-infused structured surfaces with exceptional anti-biofouling performance *Proc. Natl Acad. Sci.* **109** 13182–7
[4] Srinivasan A and Bandyopadhyay S 2016 *Advances in Polymer Materials and Technology* (Boca Raton, FL: CRC Press)
[5] Karis T E, Kim W T and Jhon M S 2005 Spreading and dewetting in nanoscale lubrication *Tribol. Lett.* **18** 27–41
[6] Popescu M N, Oshanin G, Dietrich S and Cazabat A M 2012 Precursor films in wetting phenomena *J. Phys.: Condens. Matter* **24** 243102
[7] Noble B A, Mate C M and Raeymaekers B 2017 Spreading kinetics of ultrathin liquid films using molecular dynamics *Langmuir* **33** 3476–83
[8] Noble B A, Ovcharenko A and Raeymaekers B 2016 Terraced spreading of nanometer-thin lubricant using molecular dynamics *Polymer* **84** 286–92
[9] Noble B, Ovcharenko A and Raeymaekers B 2014 Quantifying lubricant droplet spreading on a flat substrate using molecular dynamics *Appl. Phys. Lett.* **105** 151601
[10] Zhang H, Mitsuya Y and Yamada M 2003 Spreading characteristics of molecularly thin lubricant on surfaces with groove-shaped textures: effects of molecular weight and end-group functionality *J. Tribol.* **125** 350
[11] Khare K, Zhou J and Yang S 2009 Tunable open-channel microfluidics on soft poly(dimethylsiloxane) (PDMS) substrates with sinusoidal grooves *Langmuir* **25** 12794–9
[12] Zhang H, Mitsuya Y and Yamada M 2002 Spreading characteristics of molecularly thin lubricant on surfaces with groove-shaped textures: Monte Carlo simulation and measurement using PFPE film *J. Tribol.* **124** 575
[13] Hirvi J T and Pakkanen T A 2007 Wetting of nanogrooved polymer surfaces *Langmuir* **23** 7724–9
[14] Kim P, Kreder M J, Alvarenga J and Aizenberg J 2013 Hierarchical or not? Effect of the length scale and hierarchy of the surface roughness on omniphobicity of lubricant-infused substrates *Nano Lett.* **13** 1793–9
[15] Tan A H and Cheng S W 2006 A novel textured design for hard disk tribology improvement *Tribol. Int.* **39** 506–11
[16] Fukuzawa K, Deguchi T, Yamawaki Y, Itoh S, Muramatsu T and Zhang H 2008 Control of wettability of molecularly thin liquid films by nanostructures *Langmuir* **24** 2921–8
[17] Plimpton S 1995 Fast parallel algorithms for short-range molecular dynamics *J. Comput. Phys.* **117** 1–19
[18] Towns J *et al* 2014 XSEDE: accelerating scientific discovery *Comput. Sci. Eng.* **16** 62–74

[19] Guo Q, Izumisawa S, Phillips D M and Jhon M S 2003 Surface morphology and molecular conformation for ultrathin lubricant films with functional end groups *J. Appl. Phys.* **93** 8707–9
[20] Hsia Y T, Guo Q, Izumisawa S and Jhon M S 2005 The dynamic behavior of ultrathin lubricant films *Microsyst. Technol.* **11** 881–6
[21] Chen H, Guo Q and Jhon M S 2007 Effects of molecular structure on the conformation and dynamics of perfluoropolyether nanofilms *IEEE Trans. Magn.* **43** 2247–9
[22] Kocis L and Whiten W J 1997 Computational investigations of low- discrepancy sequences *ACM Trans. Math. Softw.* **23** 266–94
[23] Likhtman A E and Ponmurugan M 2014 Microscopic definition of polymer entanglements *Macromolecules* **47** 1470–81
[24] Kremer K and Grest G S 1990 Dynamics of entangled linear polymer melts: a molecular-dynamics simulation *J. Chem. Phys.* **92** 5057–86